Chapter 6
Backscattering Coefficient

The backscattered electron (BSE) emission coefficient is defined as the fraction of electrons of the primary beam emerging from the surface of an electron-irradiated target. Secondary electrons, generated in the solid by a cascade process of extraction of the atomic electrons, are not included in the definition of the backscattering coefficient. The energy cut-off is typically 50 eV. In other words, in a typical SEM experiment aimed at measuring the fraction of backscattered electrons, investigators consider as backscattered all the electrons emerging from the surface of the target with energies higher than the cut-off energy (50 eV), while all the electrons emerging with energies lower than this conventional cut-off are considered as secondary. Of course, secondary electrons with energy higher than any predefined cut-off energy and backscattered electrons with energy lower than such a cut-off also exist. If the primary energy of the incident electron beam is not too low (higher than $\approx$200–300 eV), the introduction of the 50 eV energy cut-off is generally considered as a good approximation, and it will be therefore adopted in this chapter. This choice is particularly useful, as we are interested in comparing the Monte Carlo results to experimental data that can be found in the literature, where the 50 eV energy cut-off approximation has been widely (always, actually) used.

6.1 Electrons Backscattered from Bulk Targets

When an electron beam impinges upon a solid target, some electrons of the primary beam are backscattered and re-emerge from the surface. We already know that the backscattering coefficient is defined as the fraction of the electrons of the incident beam which emerge from the surface with energy higher than 50 eV. This definition is very convenient and useful from the experimental point of view; it is also quite accurate, as the fraction of secondary electrons (i.e., the electrons extracted from the atoms of the target and able to reach the surface and emerge) with energy higher than 50 eV is negligible for any practical purpose, as is the fraction of backscattered electrons emerging with energy lower than 50 eV.

M. Dapor, *Transport of Energetic Electrons in Solids*,
Springer Tracts in Modern Physics 257, DOI 10.1007/978-3-319-47492-2_6

The backscattering coefficient of electrons in bulk targets has been studied both experimentally and theoretically. Many data, both experimental and theoretical, are available for energies higher than 5–10 keV [1, 2]. The case of energies lower than 5 keV has been investigated too, but not many experimental data are available. Furthermore, not all the authors agree about the behavior of the low energy backscattering coefficient; in particular there are very few data concerning the case in which the electron energy approaches 0. Some investigators have suggested, on the basis of experimental evidences, that the absorption coefficient should approach 0 and the backscattering coefficient should approach 1, as the energy approaches 0 [3, 4].

6.1.1 *The Backscattering Coefficient of C and Al Calculated by Using the Dielectric Theory (Ashley Stopping Power)*

If we cannot confirm that the backscattering coefficient reaches 1 as the energy approaches 0, the simulated data concerning C and Al show a general trend of the backscattering coefficient as a function of the primary energy that is consistent with this hypothesis. We have actually observed that, as the energy decreases from 10 keV to 250 eV, the simulations show that the backscattering coefficient of both C and Al increases.

In Fig. 6.1 we show the trend of the backscattering coefficient as a function of the electron beam primary energy for electrons impinging upon bulk targets of C and

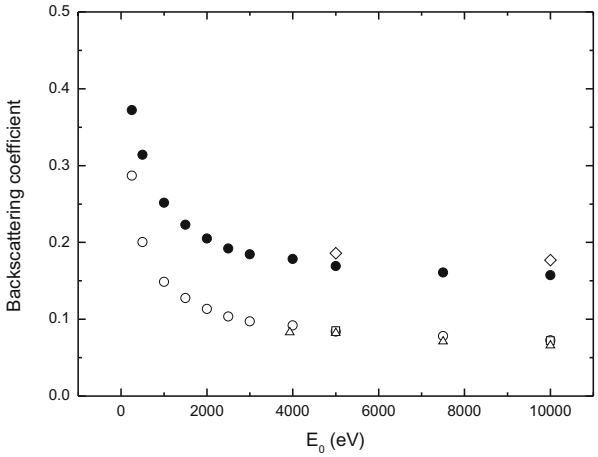

Fig. 6.1 Monte Carlo simulation of the trend of the backscattering coefficient η as a function of the electron beam primary energy E_0 for electrons impinging upon bulk targets of C (*empty circles*) and Al (*filled circles*). The stopping power was taken from Ashley [5] (dielectric theory). *Boxes* Bishop experimental data for C [6]. *Diamonds* Bishop experimental data for Al [6]. *Triangles* Hunger and Kükler experimental data for C [7]

Al as calculated by our Monte Carlo code. For the simulations presented here, the continuous-slowing-down approximation was adopted, and we calculated the stopping power by using the Ashley's recipe [5] (within the Ritchie dielectric theoretical scheme [8]). As everywhere in this book, the elastic scattering cross-section was calculated using the relativistic partial wave expansion method (Mott theory) [9]. The experimental data of Bishop [6] and Hunger and Kükler [7] are also presented in Fig. 6.1 for evaluating the accuracy of the Monte Carlo simulation.

In the case of both the examined elements, the backscattering coefficient increases as the energy decreases towards 250 eV.

6.1.2 The Backscattering Coefficient of Si, Cu, and Au Calculated by Using the Dielectric Theory (Tanuma et al. Stopping Power)

In Tables 6.1, 6.2, and 6.3 our Monte Carlo simulated data (for the backscattering coefficient of Si, Cu, and Au, respectively) are compared with the available experimental data (taken from Joy's database [10]). The Monte Carlo results were obtained using the stopping power taken from Tanuma et al. [11] (whithin the Ritchie dielectric theory [8]) for describing the inelastic processes, and the Mott theory [9] for describing the elastic scattering.

From these tables, one can observe that the backscattering coefficient is a decreasing function of the primary energy with the exception of gold, which presents an increasing trend as the energy increases in the range 1000–2000 eV. It is worth noting that the issue of the behavior of the backscattering coefficient at low primary energy is quite controversial. The reasons for the discrepancies between Monte Carlo and experimental data concerning the backscattering coefficient of low primary energy electrons, are not completely clear and deserve further investigations [16, 17]. Also,

Table 6.1 Backscattering coefficient of Si as a function of the electron primary kinetic energy. The elastic scattering cross-section was calculated using the Mott theory [9]. Continuous-slowing-down approximation was used; the stopping power was taken from Tanuma et al. [11] (dielectric theory). Comparison between the present Monte Carlo simulated results and the available experimental data (taken from Joy's database [10])

Energy (eV)	Monte Carlo	Bronstein and Fraiman [12]	Reimer and Tolkamp [13]
1000	0.224	0.228	0.235
2000	0.185	0.204	–
3000	0.171	0.192	0.212
4000	0.169	0.189	–
5000	0.162	–	0.206

Table 6.2 Backscattering coefficient of Cu as a function of the electron primary kinetic energy. The elastic scattering cross-section was calculated using the Mott theory [9]. Continuous-slowing-down approximation was used; the stopping power was taken from Tanuma et al. [11] (dielectric theory). Comparison between the present Monte Carlo simulated results and the available experimental data (taken from Joy's database [10])

Energy (eV)	Monte Carlo	Bronstein and Fraiman [12]	Koshikawa and Shimizu [14]	Reimer and Tolkamp [13]
1000	0.401	0.381	0.430	–
2000	0.346	0.379	0.406	–
3000	0.329	0.361	0.406	0.311
4000	0.317	0.340	–	–
5000	0.314	–	0.398	0.311

Table 6.3 Backscattering coefficient of Au as a function of the electron primary kinetic energy. The elastic scattering cross-section was calculated using the Mott theory [9]. Continuous-slowing-down approximation was used; the stopping power was taken from Tanuma et al. [11] (dielectric theory). Comparison between the present Monte Carlo simulated results and the available experimental data (taken from Joy's database [10])

Energy(eV)	Monte Carlo	Bronstein and Fraiman [12]	Reimer and Tolkamp [13]	Böngeler et al. [15]
1000	0.441	0.419	–	–
2000	0.456	0.450	–	0.373
3000	0.452	0.464	0.415	0.414
4000	0.449	0.461	–	0.443
5000	0.446	–	0.448	0.459

not all the experiments agree about the behavior of the low-energy backscattering coefficient in the range 1–3 keV [10].

6.2 Electrons Backscattered from One Layer Deposited on Semi-infinite Substrates

It is well known that over-layer films affect the electron backscattering coefficient of bulk targets. The experimental data available in the literature for backscattering coefficient are rather sparse and, sometimes, difficulties arise in their interpretation due to the lack of knowledge of the thickness, uniformity, and nature of the surface layers. In particular, a quantitative treatment of the effect of surface films deposited on bulk targets and a systematic comparison with experimental data are not available at the time being. The main ingredient of the present approach is the evaluation of the backscattered electron emission coefficient — that results from the interplay

between average atomic number and interaction volume — as compared to the actual thickness of the over-layer [18–21].

6.2.1 Carbon Overlayers (Ashley Stopping Power)

Let's start with the study of the low energy backscattering coefficient for the special case of layers of carbon deposited on aluminum [18].

Carbon films are deposited on various substrates (polymers, polyester fabrics, polyester yarns, metal alloys) both for experimental and technological motivations. There are a lot of technological uses of carbon films, as carbon characteristics are very useful in many fields. Carbon films deposited on polymeric substrates can be used to replace the metallic coatings on plastic materials used for food packaging. Carbon films are also widely employed in medical devices. Biomedical investigators have demonstrated that permanent thin films of pure carbon show an excellent haemo/biocompatibility: they are used, in particular, as coating for the stainless steel stents to be implanted in coronary arteries.

When investigating the behavior of the backscattering coefficient as a function of the primary energy for various film thicknesses, the appearance, for carbon film thicknesses exceeding ∼100 Å on aluminum, of relative minima can be observed. These features are presented in Fig. 6.2 for a carbon film 400 Å -thick and in Fig. 6.3 for a carbon film 800 Å -thick. The backscattering coefficient reaches a relative minimum and then increases up to the aluminum backscattering coefficient. It then follows the decreasing trend typical of the backscattering coefficient of aluminum. An interesting characteristic of the relative minima is that their position shifts towards higher energies as the film thickness increases. This is quite reasonable because one expects that, in some way, the backscattering coefficient of the system should approach the behavior of the backscattering coefficient of aluminum for very thin carbon films and should approach the energy dependence of the backscattering coefficient of carbon for thick carbon films. So, as the film thickness increases, the positions of the relative minima shift towards higher energies while the peaks broaden.

The linear best fit of the behaviour of the Monte Carlo simulated position of the relative minimum $E_{\min}$ (in eV) of the backscattering curve as a function of the film thickness t (in Å)—for C thin films deposited on an Al substrates in the range 100–1000 Å–is given by $E_{\min} = m\,t + q$, where $m = (2.9 \pm 0.1)$ eV/Å and $q = (900 \pm 90)$ eV [22].

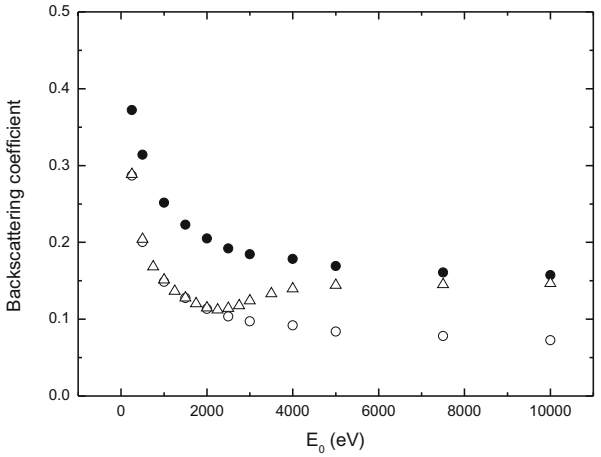

Fig. 6.2 *Triangles*: Monte Carlo simulation of the electron backscattering coefficient η for a carbon film 400 Å thick as a function of the beam primary energy E_0. *Empty circles* Monte Carlo backscattering coefficient of pure C. *Filled circles* Monte Carlo backscattering coefficient of pure Al. The stopping power was taken from Ashley [5] (dielectric theory)

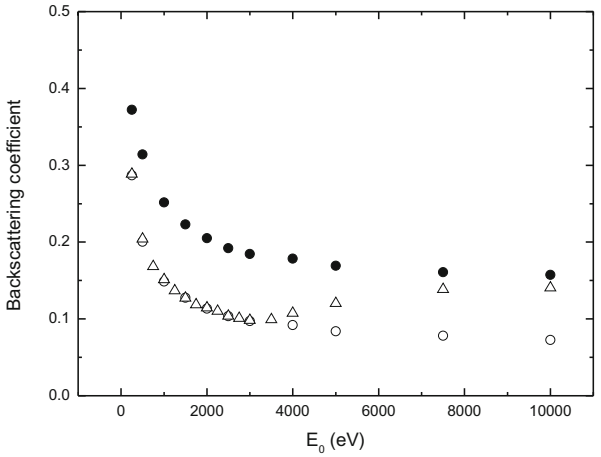

Fig. 6.3 *Triangles*: Monte Carlo simulation of the electron backscattering coefficient η for a carbon film 800 Å thick as a function of the beam primary energy E_0. *Empty circles* Monte Carlo backscattering coefficient of pure C. *Filled circles* Monte Carlo backscattering coefficient of pure Al. The stopping power was taken from Ashley [5] (dielectric theory)

6.2.2 *Gold Overlayers (Kanaya and Okayama Stopping Power)*

The behavior described above has been observed both numerically [18–22] and experimentally [20, 21] also for other materials. In all the cases, the backscattering coefficient of the system ranges from the value of the backscattering coefficient of the overlayer (for very low primary energy) to the value of the backscattering coefficient of the substrate (for very high primary energy). In the case of gold deposited on silicon, the backscattering coefficient reaches a relative maximum and then decreases to the silicon backscattering coefficient. In general, the backscattering coefficient of any system should resemble the behavior of the backscattering coefficient of the substrate for very thin films and approach the behavior of the backscattering coefficient of the material constituting the overlayer for thick films. So, as the film thickness increases, the position of the relative maximum (or minimum, depending on the constituting materials of overlayer and substrate) shifts towards higher energies while the peaks broaden [18, 19, 21, 22].

Figures 6.4 and 6.5 display the data points for the experimental backscattering coefficient and the relevant Monte Carlo results for two samples of gold layers deposited on silicon [21]. The nominal thickness of the gold films were, respectively, 250 and 500 Å. Data were normalized by dividing the curves by their respective maxima. The experimental and the Monte Carlo approaches provide similar results.

Similarly to the case of carbon on aluminum, Monte Carlo simulations predict that the energy position of the maximum, E_{max}, linearly depends on the gold overlayer thickness. The linear best fit of E_{max} as a function of the Au film thickness for

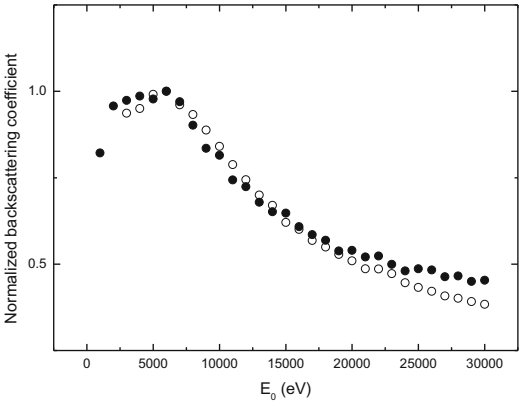

Fig. 6.4 Comparison between normalized experimental and present Monte Carlo backscattering coefficient as a function of the primary electron energy of an Au thin film deposited on a Si substrate [21]. *Empty symbols* experiment. *Filled symbols* Monte Carlo. The Au overlayer nominal thickness is 250 Å. Stopping power was calculated by using the Kanaya and Okayama semi-empiric formula [23]. Layer deposition: *courtesy* of Michele Crivellari. Experimental data: *courtesy* of Nicola Bazzanella and Antonio Miotello

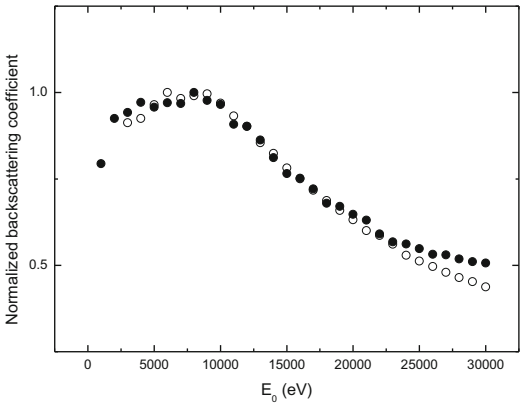

Fig. 6.5 Comparison between normalized experimental and present Monte Carlo backscattering coefficient as a function of the primary electron energy of an Au thin film deposited on a Si substrate [21]. *Empty symbols* experiment. *Filled symbols* Monte Carlo. The Au overlayer nominal thickness is 500 Å. Stopping power was calculated by using the Kanaya and Okayama semi-empiric formula [23]. Layer deposition: *courtesy* of Michele Crivellari. Experimental data: *courtesy* of Nicola Bazzanella and Antonio Miotello

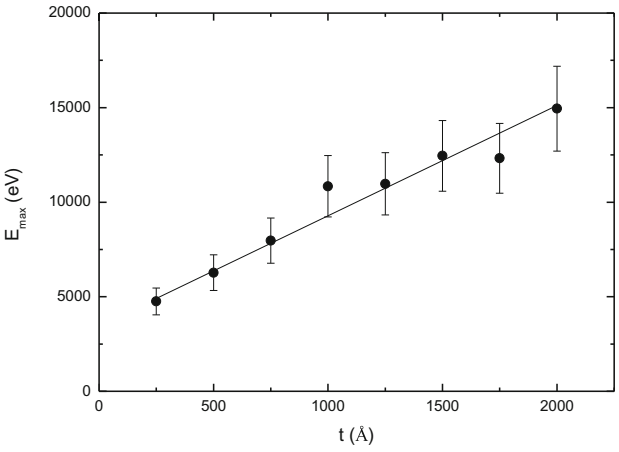

Fig. 6.6 Linear best fit of Monte Carlo simulated $E_{\max}$ (in eV) as a function of the film thickness t (in Å) for Au thin films deposited on a Si substrates in the range 250 Å-2000 Å [21]. $E_{\max} = m\,t + q$, where $m = 5.8$ eV/Å (standard error = 0.4 eV/Å) and $q = 3456$ eV (standard error = 373 eV) [21]

Au/Si systems is presented in Fig. 6.6 demonstrating that the Monte Carlo method makes it possible to evaluate the overlayer film thickness with nearly 20% uncertainty (estimated from the statistical fluctuations in the energy maximum) [21].

In view of the non-destructiveness, the proposed approach is definitely adding new potentiality to SEM-based experimental methods.

6.3 Electrons Backscattered from Two Layers Deposited on Semi-infinite Substrates

We are now interested in the calculation of the backscattering coefficient from two layers of different materials and thicknesses deposited on semi-infinite substrates. In particular, we will examine the backscattering from Cu/Au/Si and C/Au/Si systems.

In Fig. 6.7, Monte Carlo electron backscattering coefficient of Cu/Au/Si samples is represented. The Monte Carlo simulation code considers the Si substrate as a semi-infinite bulk, while the thickness of the intermediate Au layer is set at 500 Å. The behavior of η as a function of the primary energy, in the 1000–25000 eV range, is represented for different values of the Cu first layer thickness, in the 250–1000 Å range. Stopping power is calculated using the dielectric response theory.

Figure 6.8 shows the same quantities, obtained with the same conditions and calculated with the Monte Carlo code based on the Kanaya and Okayama semi-empiric formula.

The general trends obtained with the two codes are in good qualitative agreement: both codes predict that the general structure of the curves presents a minimum and a maximum. Furthermore both the minimum and the maximum shift towards higher primary energies as the Cu first layer thickness increases. Thus, this behavior is typical of the particular combination of the selected materials and of their thicknesses.

In order to further investigate and better understand the effects of layer thickness, in Figs. 6.9 and 6.10 the Monte Carlo backscattering coefficients, obtained with the dielectric response and the semi-empiric approach, respectively, have been repre-

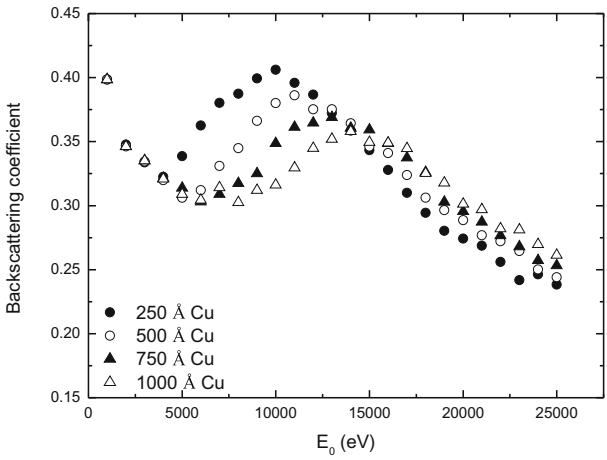

Fig. 6.7 Present Monte Carlo simulation of electron backscattering coefficient η of Cu/Au/Si samples. The Si substrate is semi-infinite, while the thickness of the intermediate Au layer is 500 Å. The behavior of η as a function of the primary energy is represented for different values of the Cu first layer thickness. Stopping power is calculated using the dielectric response theory

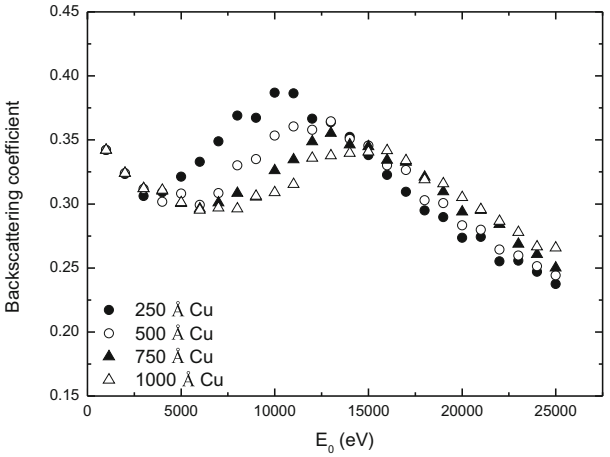

Fig. 6.8 Present Monte Carlo simulation of electron backscattering coefficient η of Cu/Au/Si samples. The Si substrate is semi-infinite, while the thickness of the intermediate Au layer is 500 Å. The behavior of η as a function of the primary energy is represented for different values of the Cu first layer thickness. Stopping power is calculated using the Kanaya and Okayama semi-empiric formula

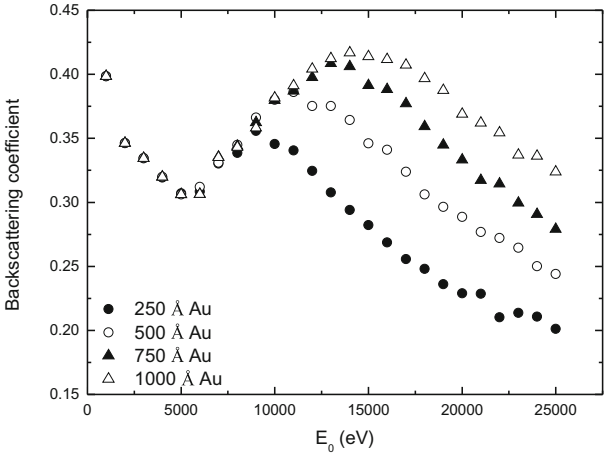

Fig. 6.9 Present Monte Carlo simulation of electron backscattering coefficient η of Cu/Au/Si samples. The Si substrate is semi-infinite, while the thickness of the first Cu layer is 500 Å. The behavior of η as a function of the primary energy is represented for different values of the Au intermediate layer thickness. Stopping power is calculated using the dielectric response theory

sented for the case in which the thickness of the first Cu layer is fixed (500 Å) while the intermediate Au film thickness ranges in the 250–1000 Å interval. Also in this case, the general behaviors obtained with the two approaches are in good qualitative agreement. The characteristic features present a trend different with respect to

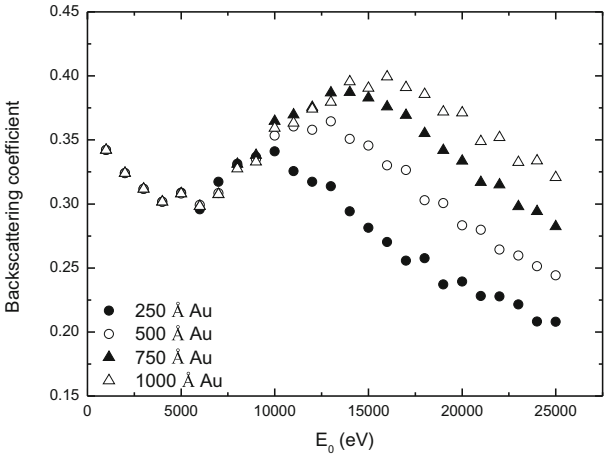

Fig. 6.10 Present Monte Carlo simulation of electron backscattering coefficient η of Cu/Au/Si samples. The Si substrate is semi-infinite, while the thickness of the first Cu layer is 500 Å. The behavior of η as a function of the primary energy is represented for different values of the Au intermediate layer thickness. Stopping power is calculated using the Kanaya and Okayama semi-empiric formula

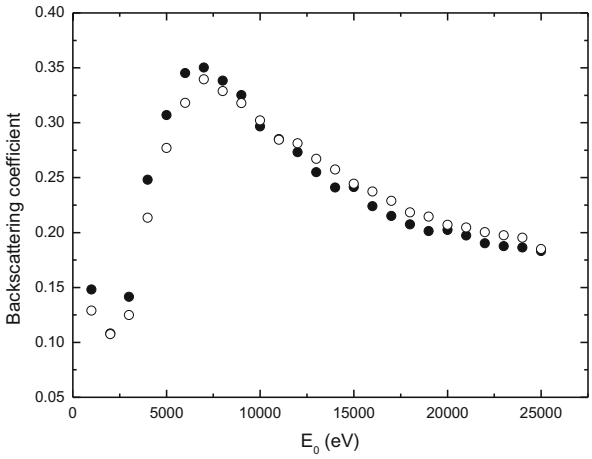

Fig. 6.11 Present Monte Carlo simulation of electron backscattering coefficient η of C/Au/Si samples. The Si substrate is semi-infinite, the thickness of the first C layer is 500 Å, and that of the intermediate Au layer is 250 Å. Backscattering coefficients η obtained using the dielectric response theory (*filled symbols*) and the semi-empiric Kanaya and Okayama approach (*empty symbols*), respectively, for calculating the stopping power, are compared

the previous one: while the position of the maximum shifts toward higher primary energies as the intermediate film thickness increases, the position of the minimum remains practically unchanged.

In order to study the agreement between the two codes, Figs. 6.11, 6.12 and 6.13 compare the calculation of the backscattering coefficients for various combinations of materials and thicknesses, obtained using the two Monte Carlo programs. The codes give practically indistinguishable results for the cases corresponding to the C/Au/Si

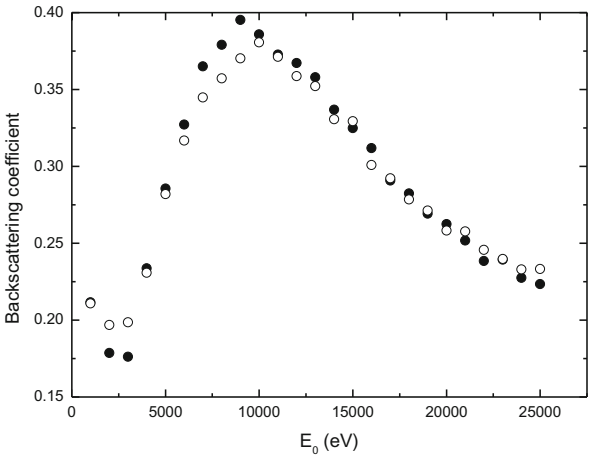

Fig. 6.12 Present Monte Carlo simulation of electron backscattering coefficient η of Al/Au/Si samples. The Si substrate is semi-infinite, the thickness of the first Al layer is 500 Å, and that of the intermediate Au layer is 500 Å. Backscattering coefficients η obtained using the dielectric response theory (*filled symbols*) and the semi-empiric Kanaya and Okayama approach (*empty symbols*), respectively, for calculating the stopping power, are compared

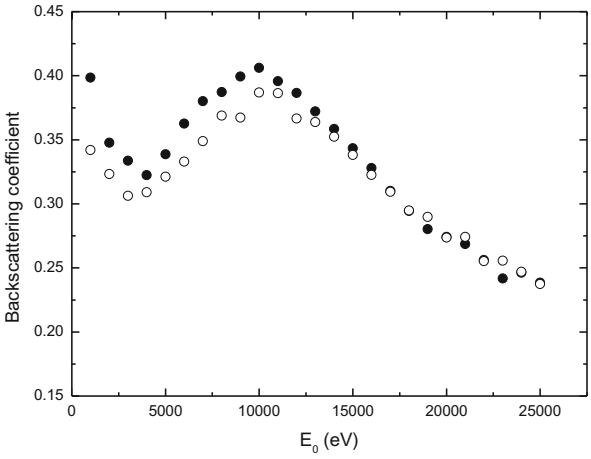

Fig. 6.13 Present Monte Carlo simulation of electron backscattering coefficient η of Cu/Au/Si samples. The Si substrate is semi-infinite, the thickness of the first Cu layer is 250 Å, and that of the intermediate Au layer is 500 Å. Backscattering coefficients η obtained using the dielectric response theory (*filled symbols*) and the semi-empiric Kanaya and Okayama approach (*empty symbols*), respectively, for calculating the stopping power, are compared

combination, while some difference can be observed, for the lowest energies, in the case of the Cu/Au/Si combinations.

6.4 A Comparative Study of Electron and Positron Backscattering Coefficients and Depth Distributions

To conclude this chapter, we will compare the Monte Carlo simulations of the backscattering coefficients and the depth distributions of electrons and positrons. Just to provide an example, we will consider the case of penetration of electrons and positrons in silicon dioxide. The presented results were obtained using the Ashley

theory for calculating the stopping power and the Mott cross-section for the computation of the differential elastic scattering cross-section [24].

The differences in the inelastic and elastic scattering cross-sections of low energy electrons and positrons, discussed in Chap. 3 and in Chap. 11, explain the results presented in Fig. 6.14. The depth profiles of electrons and positrons are different even for the highest energy examined (10 keV), for each particle reduces its energy during its travel in the solid, reaching the low values corresponding to significant differences in the cross-sections and stopping powers of electrons and positrons.

Indicating with $R(E_0)$ the maximum penetration range, for any given energy E_0, R can be easily determined by the curves in Fig. 6.14. From the presented depth profiles it is clear that the maximum penetration range in silicon dioxide is approximately the same for electrons and positrons, in the examined primary energy range.

For each primary energy E_0, the integration of the function $P(z)$ from $z = 0$ to $z = R$ gives the absorption coefficient $1 - \eta(E_0)$, where we indicated with $\eta(E_0)$ the backscattering coefficient. As the primary energy increases, the differences in the depth distributions of electrons and positrons grow smaller. While the maximum ranges of electrons and positrons are similar, the backscattering coefficients present very different trends (see Fig. 6.15). The positron backscattering coefficient does not depend on the primary energy and is always smaller than the electron backscattering coefficient. Instead, the electron backscattering coefficient is a decreasing function of the primary energy.

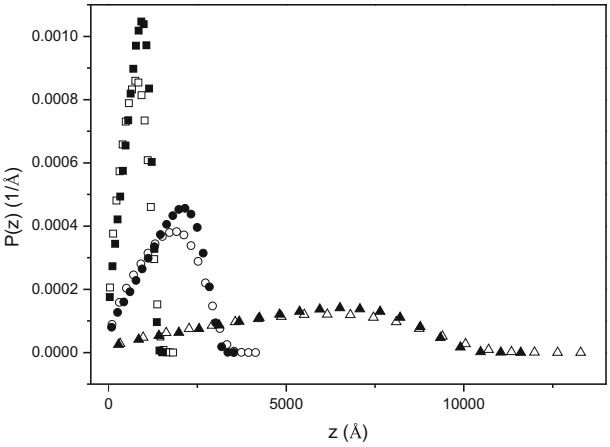

Fig. 6.14 Monte Carlo simulation of the depth profiles $P(z)$ of electrons (*empty symbols*) and positrons (*filled symbols*) in SiO_2 as a function of the depth inside the solid measured from the surface, z. E_0 is the primary energies of the particles. 3 keV (*squares*), 5 keV (*circles*) and 10 keV (*triangles*)

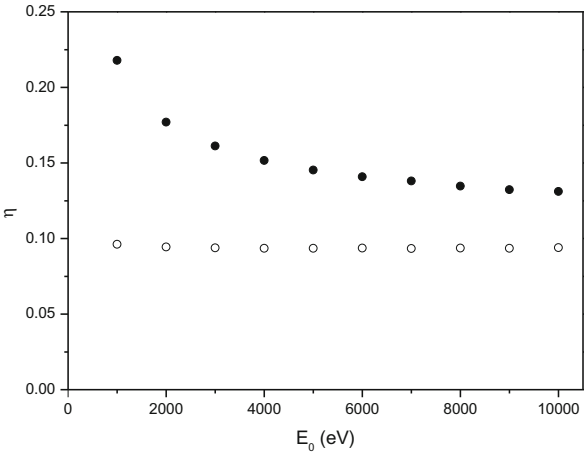

Fig. 6.15 Monte Carlo simulation of the backscattering coefficient η of electrons (*filled symbols*) and positrons (*empty symbols*) in SiO_2 as a function of the primary energy E_0

6.5 Summary

In this chapter, the Monte Carlo method was used for evaluating the backscattering coefficient of electrons (and positrons) impinging upon bulks and overlayers. In particular, for the case of surface films, it was calculated as a function of the thicknesses of the layers, their nature, and the electron primary energy. The code used in this chapter, utilizes the Mott cross-section for elastic scattering calculation and the continuous-slowing-down approximation for energy loss simulation. For the calculation of the stopping power, the Ritchie dielectric response theory [8] and the analytic semi-empirical formula proposed by Kanaya and Okayama [23] were used. Electron backscattering coefficients from several different combinations of layers and substrates were simulated. The main features of the backscattering coefficient as a function of the electron primary energy, which are represented by minima and maxima whose positions in energy depend on the particular combination of materials and thicknesses, are reproduced in similar ways using the two different stopping powers. The last section of this chapter presented a comparative study of electron and positron depth distributions and backscattering coefficients.

References

1. M. Dapor, Phys. Rev. B **46**, 618 (1992)
2. M. Dapor, *Electron-Beam Interactions with Solids: Application of the Monte Carlo Method to Electron Scattering Problems* (Springer, Berlin, 2003)
3. R. Cimino, I.R. Collins, M.A. Furman, M. Pivi, F. Ruggiero, G. Rumolo, F. Zimmermann, Phys. Rev. Lett. **93**, 014801 (2004)
4. M.A. Furman, V.H. Chaplin, Phys. Rev. Spec. Top. Accel. Beams **9**, 034403 (2006)
5. J.C. Ashley, J. Electron Spectrosc. Relat. Phenom. **46**, 199 (1988)

6. H.E. Bishop, Proc. 4ème Congrès International d'Optique des Rayons X et de Microanalyse pp. 153–158 (1967)
7. H.J. Hunger, L.G. Küchler, Phys. Status Solidi A **56**, K45 (1979)
8. R.H. Ritchie, Phys. Rev. **106**, 874 (1957)
9. N.F. Mott, Proc. R. Soc. Lond. Ser. **124**, 425 (1929)
10. D.C. Joy, (2008). http://web.utk.edu/srcutk/htm/interact.htm
11. S. Tanuma, C.J. Powell, D.R. Penn, Surf. Interface Anal. **37**, 978 (2005)
12. I.M. Bronstein, B.S. Fraiman, *Vtorichnaya Elektronnaya Emissiya* (Nauka, Moskva, 1969)
13. L. Reimer, C. Tolkamp, Scanning **3**, 35 (1980)
14. T. Koshikawa, R. Shimizu, J. Phys. D. Appl. Phys. **6**, 1369 (1973)
15. R. Böngeler, U. Golla, M. Kussens, R. Reimer, B. Schendler, R. Senkel, M. Spranck, Scanning **15**, 1 (1993)
16. J. Ch, Kuhr, H.J. Fitting, Phys. Status Solidi A **172**, 433 (1999)
17. M.M. El Gomati, C.G. Walker, A.M.D. Assa'd, M. Zadražil, Scanning **30**, 2 (2008)
18. M. Dapor, J. Appl. Phys. **95**, 718 (2004)
19. M. Dapor, Surf. Interface Anal. **40**, 714 (2008)
20. M. Dapor, N. Bazzanella, L. Toniutti, A. Miotello, S. Gialanella, Nucl. Instrum. Methods Phys. Res. B **269**, 1672 (2011)
21. M. Dapor, N. Bazzanella, L. Toniutti, A. Miotello, M. Crivellari, S. Gialanella, Surf. Interface Anal. **45**, 677 (2013)
22. M. Dapor, Surf. Interface Anal. **38**, 1198 (2006)
23. K. Kanaya, S. Okayama, J. Phys. D. Appl. Phys. **5**, 43 (1972)
24. M. Dapor, J. Electron Spectrosc. Relat. Phenom. **151**, 182 (2006)